PROCEEDINGS OF THE INTERNATIONAL CONFERENCE NANOMATERIALS: APPLICATIONS AND PROPERTIES
Vol. **1** No 1, 01PCN04(4pp) (2012)

Structural Characterization of Colloidal Core-shell Polymer-based Nanoparticles Using Small-angle X-ray Scattering

O.O. Mykhaylyk*

Department of Chemistry, University of Sheffield, Sheffield, S3 7HF, United Kingdom

(Received 19 May 2012; published online 16 August 2012)

Colloidal particle complexes are often characterized by small angle X-ray scattering (SAXS) techniques. The present work demonstrates SAXS analysis of inhomogeneous core-shell nanoparticles with complex shell morphologies. Different experimental techniques such as variation of particle composition and contrast variation method, and analytical techniques such as Monte Carlo simulation and indirect Fourier transformation are applied to obtain structural parameters of polymer-based core-shell nanoparticles. It is shown that the SAXS results are consistent with other measurements performed by electron microscopy, atomic force microscopy, dynamic light scattering, thermogravimetry, helium pycnometry and BET.

Keywords: SAXS, polymers, self-assembled nanostructures, distance distribution function.

DOI: PACS number(s): 61.05.cf, 61.46.-w

1. INTRODUCTION

A significant amount of structures existing in nature could be classified as a core-shell structure where the shell is usually formed as a result of interaction between the body and the surrounding medium and functioning as a protecting barrier between the body and the rest of the world. Another example, mimicking the nature, is synthetic colloidal core-shell nanocomposite particles which have numerous applications, including drug delivery [1], photonic devices [2], or high performance coatings [3]. Amongst these examples a dominating position is occupied by core-shell particles with spherical symmetry represented by vesicles [4], liposome [5], micelles [6], latex particles [7], viruses [8] and even inorganic nanoparticles [9].

Two different approaches are usually used in structural characterization of the core-shell particles: microscopy (electron microscopy, scanning microscopy and/or atomic force microscopy) and scattering (dynamic light scattering, neutron scattering and/or X-ray scattering). In spite of the fact that microscopy is an effective tool for structural characterization at nanoscale there is often an advantage in the application of integrating and non-destructive scattering techniques. In this respect small-angle X-ray scattering (SAXS) is a highly informative method for characterizing core-shell particles. SAXS of systems containing inhomogeneous particles can be treated using a model describing the particle shape and their internal structure. The form factor for various inhomogeneous particles, such as spherical, elliptical, cylindrical and sphero-cylindrical concentric shells with different scattering density are available in a full- or semi-analytical form [10]. However, the difficulties in the interpretation of scattering functions obtained from experiment are caused by the highly abstract nature of reciprocal space. A serious progress in SAXS analysis has been made with development of indirect methods where SAXS patterns available from experiment in only a limited region of q-values are used to calculate the distance distribution function of particles $p(r)$ [11,12]. The main advantage of $p(r)$ over scattering functions in interpretation of SAXS results is that they represent a structure in a real space. Inhomogeneous particles with at least two regions of electron densities differing in their sign, with respect to the scattering medium, show distinctive features in the distance distribution [13]. If shapes of inhomogeneous objects are known the $p(r)$ can be effectively used to study the inner structure of the objects, in particular, core-shell structures where real systems may have size polydispersity of both the core and the thickness of the shell, deviations in densities of the core and/or the shell including extra phase separation in the core and/or the shell of the particles.

In this work a comprehensive SAXS analysis of core-shell particles using both approaches, a reciprocal space (scattering patterns) and a real space (distance distribution functions), is presented. SAXS analysis of a series of poly(styrene-co-*n*-butyl acrylate)/silica colloidal nanocomposite particles was carried out to demonstrate an application of the reciprocal space approach in structural characterization of complex core-particulate shell nanostructures. [14] A set of distance distribution functions calculated from SAXS patterns of latex core-shell particles obtained by the contrast variation method is used to demonstrate an effectiveness of real-space $p(r)$ functions in an interpretation of inner structure of core-shell particles. [15]

2. METHOD AND MATERIALS

2.1 SAXS Measurements

SAXS patterns were recorded at Synchrotron Radiation Source, CCLRC Daresbury Laboratory, UK on stations 2.1 and 16.1 in a q-range 0.004-0.07 Å^{-1} (scattering wave vector $q = 4\pi\sin\theta/\lambda$, where θ is a half of scattering angle) using a two-dimensional area detector RAPID. All measurements have been carried

* O.Mykhaylyk@sheffield.ac.uk

out at room temperature. A liquid cell comprised of two mica windows (each of 25 microns thickness) separated by a polytetrafluoroethylene spacer of 1 mm thickness has been used as a sample holder. Peak positions of a wet rat-tail collagen have been used to calibrate the *q*-axis of the SAXS patterns. Two-dimensional SAXS patterns have been reduced to one-dimensional profiles by a standard procedure available in the BSL software package (http://www.small-angle.ac.uk/).

2.2 Materials

Poly(styrene-co-*n*-butyl acrylate)/silica colloidal core/particulate shell nanocomposite particles were prepared by the in situ emulsion copolymerization of styrene and *n*-butyl acrylate in the presence of a glycerol-functionalized silica sol (Fig. 1). The resulting milky-white colloidal dispersions were purified by repeated centrifugation-redispersion cycles (5,000-7,000 rpm for 30 min) using a refrigerated centrifuge (cooled to 5 °C). [14]

The core-shell latex particles of polymethylmethacrylate (PMMA) and polyurethane (PU) of various sizes have been synthesised by mini-emulsion polymerisation of MMA in a self-emulsifying dispersion of PU (Fig. 2). A set of 2 vol% water sucrose solutions of the latex particles has been prepared for SAXS contrast variation measurements. The electron density of the aqueous medium was raised by adding certain amounts of D(+)-sucrose.

The polyurethane, comprising the shell, is phase-separated into hard and soft blocks via spinodal decomposition. Some evidence of the PU phase separation can be found in the AFM image of this material (Fig. 2B), where disk-like domains evenly distributed over the surface of the particles with inter-domain distances in a range of 100-200 Å (compare models in Fig. 2C and 2D). The spinodal decomposition wave is confined by the shell and can only propagate along the surface of the particles.

3. RESULTS AND DISCUSSION

3.1 Reciprocal Space Analysis

A two-population model based on standard SAXS equations was verified for the analysis of core-shell structures comprising spherical colloidal particles with particulate shells. [14] The first population of the model, the core-shell structure, describes the self-correlation term of the spherical polymer core and the cross-term between the core and the particles within the shell. The second population describes the self-correlation term for the particulate shell and also the cross-term between these packed particles. This approach provides sufficient flexibility to model the size distributions of both the large core particles and the smaller particles within the shell. Moreover, it also provides an opportunity to account for the nature of the inter-particle interactions within the shell by exploring different structure factors. First, Monte Carlo simulations of core-shell structures were performed to demonstrate the applicability of the model. Two possible shell packings were considered: randomly-arranged silica particles (Fig. 1C) and ordered silica

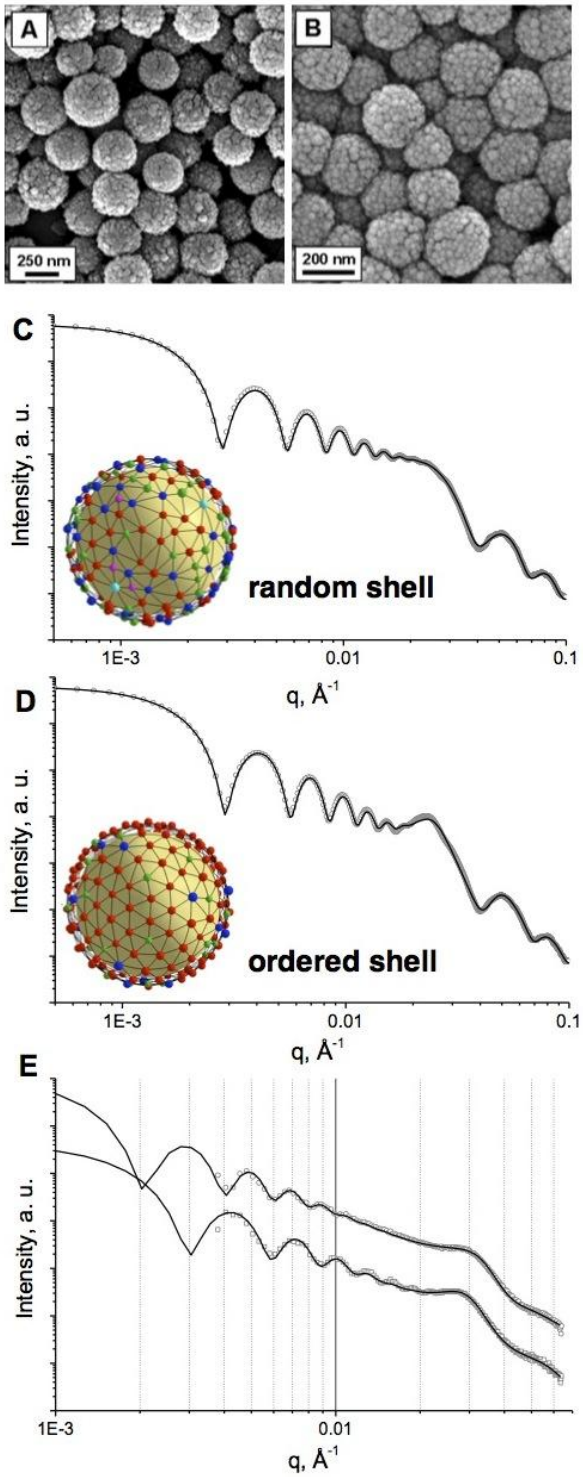

Fig. 1 – Scanning electron microscopy of polystyrene/silica (A) and 70:30 poly(styrene-*stat*-*n*-butyl acrylate) copolymer/silica nanocomposite core/shell particles. Calculated SAXS patterns (symbols) and corresponding fittings using the two-population model (lines) for simulated core-particulate shell particles comprising polystyrene cores and silica particles with a packing density D = 0.45 distributed randomly within the shell (C) and distributed uniformly using repulsive interactions (D). SAXS profiles (symbols) and corresponding fittings using the two-population model (lines) obtained for 0.50 wt% aqueous dispersions of 70:30 poly(styrene-*stat*-*n*-butyl acrylate)/silica (squares) and polystyrene/silica (circles) nanocomposite particles (E). For clarity, the last pattern was multiplied by a factor of 10.

shells due to charge-dependent repulsive interactions (Fig. 2D). In most cases the two-population model produces an excellent fit to calculated SAXS patterns for the simulated core-shell structures, together with a good correlation between the fitting parameters and structural parameters used for the simulation (Fig. 1C and 1D). The two-population model can be applied for structural analysis of core-particulate shell particles formed by evenly-distributed silica (i.e. repulsive interactions) over a wide range of silica concentrations from a dense packing, close to the theoretical limits, to packing values as low as $D = 0.09$. However, the model has limits for randomly-ordered shells at low silica concentrations.

The two-population model has been used further for structural characterization of a series of poly(styrene-co-*n*-butyl acrylate)/silica colloidal nanocomposite particles (Fig. 1E). The overall core-shell particle diameter, the copolymer latex core diameter and polydispersity, the mean silica shell thickness, the mean silica diameter and polydispersity, the volume fractions of the two components, the silica packing density and the silica shell structure obtained from this SAXS analysis were consistent with other techniques (electron microscopy, dynamic light scattering, thermogravimetry, helium pycnometry and BET surface area studies) [14].

3.2 Real Space Analysis

SAXS patterns of PMMA/PU particles have been obtained using contrast variation technique (Fig. 2E). Indirect methods have been applied to calculate distance distribution functions from SAXS (Fig. 2F), for latexes dissolved in various sucrose solutions over a range of solution density yielding structural parameters of the particles such as core size, shell thickness and density of the polymers. It is demonstrated that distance distribution functions obtained for the latex particles diluted in water sucrose solutions, in a range of electron densities matching those of the polymers comprising the core-shell particles is sensitive to deviations in both geometrical parameters of the particles and electron density of the polymers. This effect has been used to measure the electron density deviations within the particle's core and shell. The model for an ensemble of normally distributed core-shell particles with variable average electron density of both the core and the shell has been developed to fit the distance distribution functions using a random search algorithm (Fig. 2F). The results have shown that the synthetic route used produces core-shell particles with a relatively narrow distribution of the total diameter. However, the spatial distribution of the different polymers within the particles themselves, which may form bubble-like morphologies one in another or even continuous interpenetrating networks, can vary due to the stochastic nature of the mini-emulsion process, thereby changing the average electron density of the core and the shell from one particle to another.

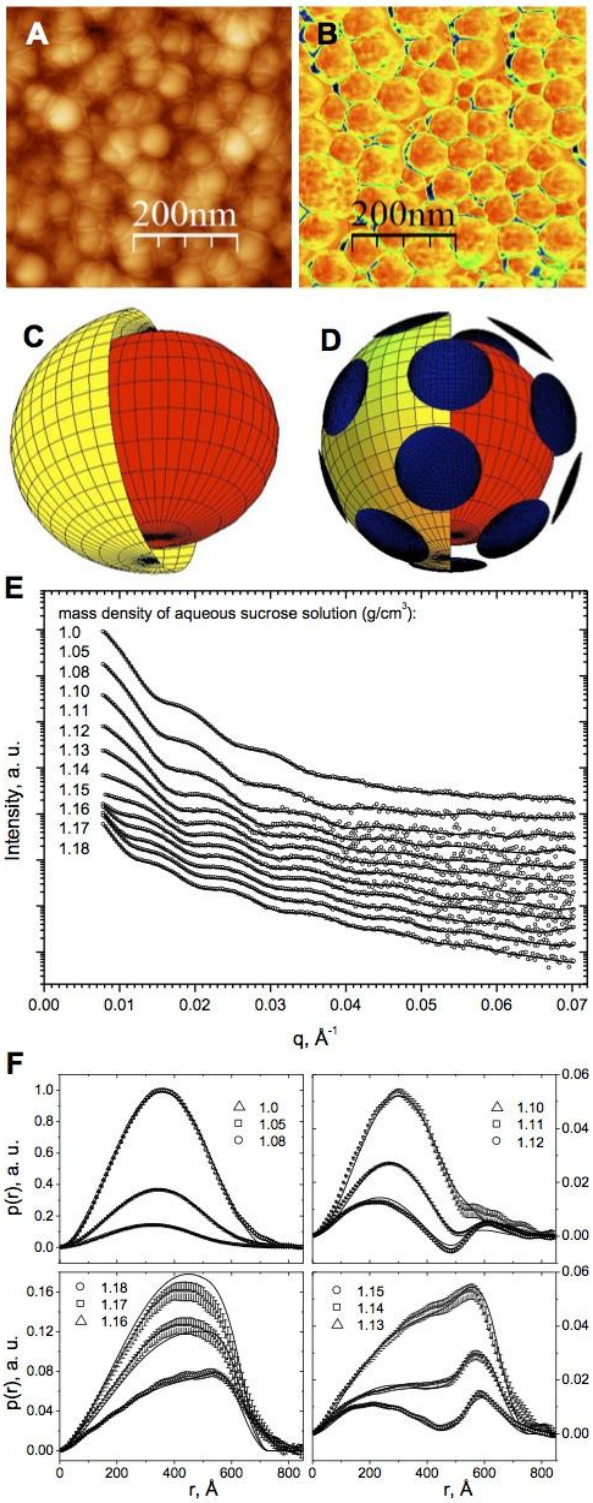

Fig. 2 – Atomic force microscopy of colloidal latex PU/PMMA core/shell particles: a topographic image, amplitude of the tip vibrations was tuned to detect the core-shell structure, (A) and a phase image (B). A model of core-shell particle (C) and a model with spherical caps evenly distributed in the shell of the particle imitating phase separation of a polymer material in the shell (D). SAXS patterns of the 2 vol. % PU/PMMA particles suspended in aqueous sucrose solutions, mass densities of the contrast solutions shown on the left-hand side of the graph, the patterns have been shifted by a factor of 2 to avoid overlapping (circles) together with scattering intensities restored by regularization technique using GNOM software

[12] (lines) (E) and corresponding distance distribution functions obtained by indirect method (symbols) fitted with the model of normal distribution of particles with variable electron densities (lines) (F). The obtained fitting parameters are: core radius R_c = 259 Å, shell thickness ΔR = 119 Å, core electron density ξ_c = 0.379 electrons/Å^3, shell electron density ξ_s = 0.366 electrons/Å^3 and their standard deviations σ_c = 0.018 electrons/Å^3 and σ_s = 0.005 electrons/Å^3.

The effects of nanophase separation in the polyurethane is estimated using Monte-Carlo simulations of the distance distribution functions where the phase-separated polyurethane is represented by spherical caps in a shell simulating the location of hard polyurethane blocks (Fig. 2D).

AKNOWLEDGEMENTS

The author is grateful to Neil Williams, Jennifer Balmer, Andreas Schmid and other coworkers whose work is published in ref. 14 and ref. 15.

REFERENCES

1. A. Sharma, U.S. Sharma, *International Journal of Pharmaceutics* **154** No2, 123 (1997).
2. D.B. Mitzi, *Chemistry of Materials* **13** No10, 3283 (2001).
3. F. Tiarks, J. Leuninger, O. Wagner, E. Jahns, H. Wiese, *Surface Coatings International* **90** No5, 221 (2007).
4. D.E. Discher, A. Eisenberg, *Science* **297** 967 (2002).
5. T. Baumgart, S.T. Hess, W.W. Webb, *Nature* **425** No6960, 821 (2003).
6. I.W. Hamley, *The Physics of Block Copolymers* (Oxford: Oxford University Press: 1998).
7. J. Bolze, M. Ballauff, J. Kijlstra, D. Rudhardt, *Macromolecular Materials and Engineering* **288** No6, 495 (2003).
8. T. Lin, Z. Chen, R. Usha, C.V. Stauffacher, J.B. Dai, T. Schmidt, J.E. Johnson, *Virology* **265** 20 (1999).
9. O.O. Mykhaylyk, Y.M. Solonin, B.D. N., R.M.D. Brydson, *Journal of Applied Physics* **97** No7, 074302 (2005).
10. J.S. Pedersen, *Advances in Colloid and Interface Science* **70** 171 (1997).
11. O. Glatter, *Journal of Applied Crystallography* **10** NoOCT1, 415 (1977).
12. D.I. Svergun, A.V. Semenyuk, L.A. Feigin, *Acta Crystallographica Section A* **44** 244 (1988).
13. O. Glatter, *Journal of Applied Crystallography* **12** NoAPR, 166 (1979).
14. J.A. Balmer, O.O. Mykhaylyk, A. Schmid, S.P. Armes, J.P.A. Fairclough, A.J. Ryan, *Langmuir* **27** No13, 8075 (2011).
15. O.O. Mykhaylyk, A.J. Ryan, N. Tzokova, N. Williams, *Journal of Applied Crystallography* **40** S506 (2007).